ELSEVIER

Surface Science 310 (1994) 198–208

surface science

A LEED, TPD and HREELS investigation of NO adsorption on Sn/Pt(111) surface alloys

Chen Xu, Bruce E. Koel *

Department of Chemistry, University of Southern California, Los Angeles, CA 90089, USA

(Received 22 October 1993; accepted for publication 14 December 1993)

Abstract

The adsorption of NO on Pt(111), and the (2×2)Sn/Pt(111) and $(\sqrt{3}\times\sqrt{3})$R30°Sn/Pt(111) surface alloys has been studied using LEED, TPD and HREELS. NO adsorption produces a (2×2) LEED pattern on Pt(111) and a $(2\sqrt{3}\times2\sqrt{3})$R30° LEED pattern on the (2×2)Sn/Pt(111) surface. The initial sticking coefficient of NO on the (2×2)Sn/Pt(111) surface alloy at 100 K is the same as that on Pt(111), $S_0 = 0.9$, while the initial sticking coefficient of NO on the $(\sqrt{3}\times\sqrt{3})$R30°Sn/Pt(111) surface decreases to 0.6. The presence of Sn in the surface layer of Pt(111) strongly reduces the binding energy of NO in contrast to the minor effect it has on CO. The binding energy of β-state NO is reduced by 8–10 kcal/mol on the Sn/Pt(111) surface alloys compared to Pt(111). HREELS data for saturation NO coverage on both surface alloys show two vibrational frequencies at 285 and 478 cm^{-1} in the low frequency range and only one N–O stretching frequency at 1698 cm^{-1}. We assign this NO species as atop, bent-bonded NO. At small NO coverage, a species with a loss at 1455 cm^{-1} was also observed on the (2×2)Sn/Pt(111) surface alloy, similar to that observed on the Pt(111) surface. However, the atop, bent-bonded NO is the only species observed on the $(\sqrt{3}\times\sqrt{3})$R30°Sn/Pt(111) surface alloy at any NO coverage studied.

1. Introduction

The adsorption of NO on transition metal surfaces has been intensively studied in the past [1–14]. These studies often have been motivated by the importance of NO reduction in pollution control by automotive exhaust catalysts. NO is isoelectronic with CO^-, and this additional electron in the anti-bonding $2\pi^*$ orbital gives rise to a much richer coordination chemistry and can strongly alter the adsorption behavior for NO compared to CO.

Bimetallic surfaces often show strongly modified chemistry compared to the single-component surface of the constituent transition metals [15,16]. Both poisoning and activation effects have been observed. As a protypical molecule, CO has been extensively studied on various bimetallic surfaces. By contrast, the results in the literature regarding adsorption of NO are rare. In this paper we report our TPD, LEED and HREELS investigation of NO on two ordered Sn/Pt(111) surface alloys. Our results show that Sn has a very different influence on NO adsorption than on CO adsorption on these surfaces. This difference has been discussed within the context of the different bonding mechanism of CO and NO on transition metals.

* Corresponding author. Fax: +1 (213) 746 4945.

SSDI 0039-6028(93)E1053-3

2. Experimental methods

The experiments were performed in an ultra-high vacuum chamber equipped for Auger electron spectroscopy (AES), low energy electron diffraction (LEED), temperature programmed desorption (TPD) and high resolution electron energy loss spectroscopy (HREELS). The system base pressure was 5×10^{-11} Torr. TPD measurements were made using a UTI 100C quadrupole mass spectrometer in line-of-sight with the sample surface and using a linear heating rate of ~ 4.5 K/s. The mass spectrometer was equipped with a shield having a small (6 mm diameter) entry hole. The crystal was always put very close (~ 1 mm) to the entry of the QMS. In order to stop electron emission from the QMS to the sample, a screen biased with -55 V was placed in front of the QMS ionizer.

The HREELS spectra were taken with a spectrometer containing single 127° cylindrical sectors in the monochromator and analyzer. All spectra were taken in specular reflection, with $\theta_{in} = \theta_{out} = 65°$ from the surface normal. The electron incident energy was 3 eV. The typical resolution used was 60 cm^{-1}.

The Pt(111) crystal could be cooled down to 95 K using liquid nitrogen or resistively heated to 1200 K. The temperature was measured by a chromel–alumel thermocouple spotwelded to the side of the crystal.

The Pt(111) crystal was cleaned using the procedure found in Ref. [17]. The (2×2)Sn/Pt(111) and $(\sqrt{3} \times \sqrt{3})$R30°Sn/Pt(111) surfaces were prepared by evaporating Sn on the clean Pt(111) surface and subsequently annealing the sample to 1000 K for 10 s. Depending upon the initial Sn coverage, the annealed surface exhibited a $p(2 \times 2)$ or $(\sqrt{3} \times \sqrt{3})$R30° LEED pattern [18]. The structure for these patterns was originally assigned to the (111) face of Pt_3Sn and a substitutional surface alloy of composition Pt_2Sn [18], and this has now been confirmed [19,20]. A schematic drawing of both alloy surfaces is shown in Fig. 1. Angle-dependent low energy ion scattering spectroscopy (LEISS) measurements using 500–1000 eV Li^+ [19] and dynamic LEED [20] studies show that surface alloys (rather than Sn adatoms) are produced and that Sn atoms are almost coplanar with the Pt atoms at the surface; Sn only protrudes $\sim 0.022 \pm 0.005$ nm above the surface. This indicates a strong interaction between Sn and Pt atoms which is also revealed by ultraviolet photoelectron spectroscopy (UPS) [21]. For brevity in this paper, the $(\sqrt{3} \times \sqrt{3})$R30°Sn/Pt(111) surface alloy and the (2×2)Sn/Pt(111) surface alloy will be referred to as the $\sqrt{3}$ alloy and (2×2) alloy, respectively.

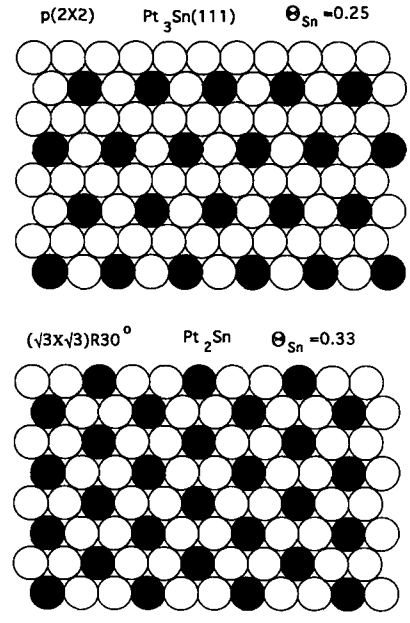

Fig. 1. Top view schematic drawing of the surface structure for the (2×2) and $(\sqrt{3} \times \sqrt{3})$R30°Sn/Pt(111) surface alloys.

NO (Matheson, 99%) was dosed using leak valves connected to collimated microcapillary array dosers. The exposures are given in units of Langmuirs (I L $= 10^{-6}$ Torr · s) uncorrected for the doser enhancement factor and ion gauge sensitivity. Adsorbate coverages in this paper are referenced to the Pt(111) surface atom density, i.e., $\theta = 1.0$ corresponds to 1.505×10^{15} atoms cm^{-2}.

3. Results

3.1. TPD

NO TPD after several NO exposures on Pt(111) and the (2×2) and $\sqrt{3}$ alloys are shown in Figs.

2–4. NO is the only measurable product desorbed at any NO coverage on all three surfaces investigated; no N_2 (mass 28), NO_2 (mass 46), N_2O (mass 40) or O_2 (mass 32) was detected by the QMS. AES measurements after TPD also show a clean surface without any oxygen or nitrogen. These results establish that NO adsorbs reversibly on all three surfaces.

On Pt(111), three desorption states can be populated with increasing NO coverages in good agreement with previous results [1–9]. The two high temperature states at 320 and 360 K have been assigned to NO desorption from two different adsorption sites: atop and bridge sites [2,7,9]. The origin of the low temperature state, however, is not clear.

Alloying the Pt(111) surface with Sn causes dramatic changes in the adsorption behavior of NO. This is clearly shown in Figs. 3 and 4. Generally speaking, a strong reduction in the NO adsorption energy occurs due to the presence of Sn in the surface alloy. On the (2 × 2) alloy, two

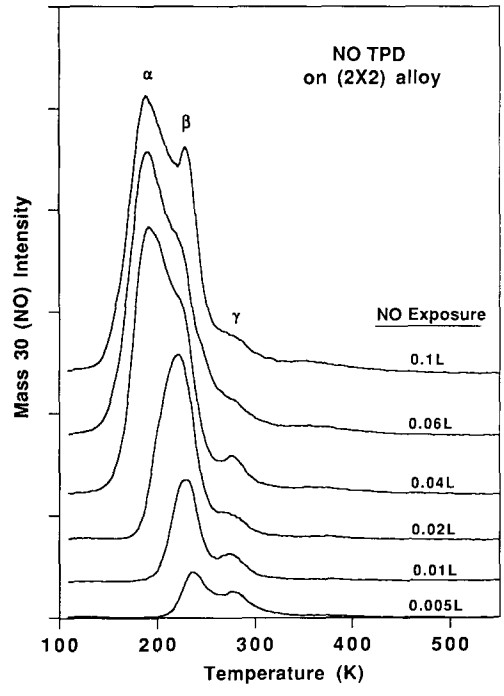

Fig. 3. NO TPD spectra after different NO exposures on the (2×2)Sn/Pt(111) surface alloy.

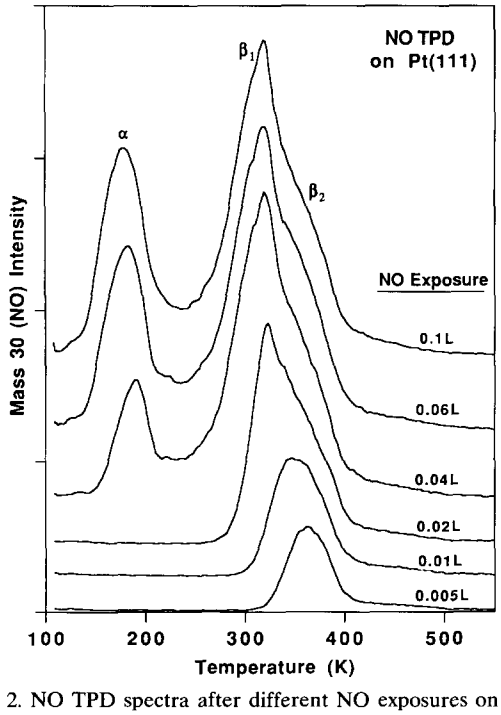

Fig. 2. NO TPD spectra after different NO exposures on the Pt(111) surface.

desorption peaks at 236 (β state) and 277 K (γ state) can be populated at lower NO coverages. With increasing amount of NO, the peak at 236 K gains intensity and shifts to lower temperature. In contrast, the peak at 277 K shows no changes with increasing NO coverage. At high NO coverages, a peak at 189 K (α state) also develops. The α state on the (2 × 2) alloy has a very similar desorption temperature to the α state on the Pt(111) surface, while the β state on the (2 × 2) alloy has a much lower desorption temperature than on the Pt(111) surface. Apparently the presence of Sn only affects the β state desorption and does not influence the α state appreciably.

Increasing the Sn concentration in the surface to 33% forms the $\sqrt{3}$ alloy and again decreases the desorption temperature of the NO β state. The β state desorption can only be observed at small NO coverage. At higher NO coverage, the β state is almost hidden by the α state and only a small asymmetry indicates its presence. Similarly to the (2 × 2) alloy, the higher temperature peak

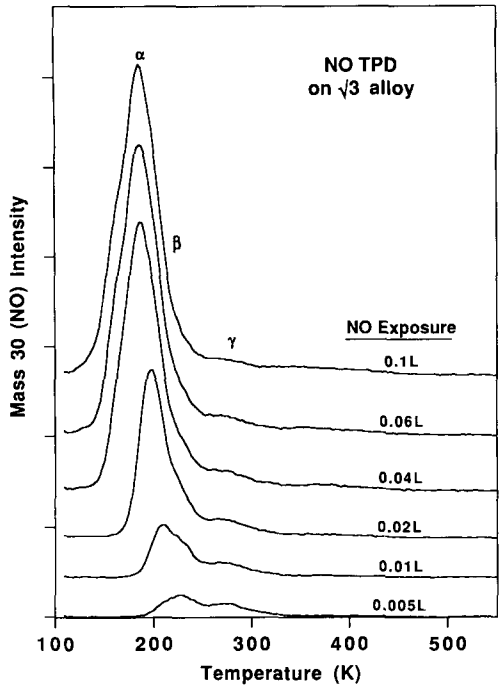

Fig. 4. NO TPD spectra after different NO exposures on the $(\sqrt{3} \times \sqrt{3})$R30°Sn/Pt(111) surface alloy.

at 277 K (γ state) can be populated on the $\sqrt{3}$ alloy. The γ state on both surface alloys has exactly the same desorption temperature and a similar intensity. This state also shows no NO-coverage dependence. We attribute this peak to desorption from defects, probably on the crystal edges. The fact that both the amount and desorption temperature of the γ state is independent of the Sn concentration in the surface gives us reason to believe that this state is not due to Pt-rich islands on the surface alloys.

The dramatic shift in desorption temperature of the most strongly bonded NO can be seen more clearly in Fig. 5, which compares TPD spectra for saturation NO coverages on Pt(111), and the (2×2) and $\sqrt{3}$ alloy surfaces. As mentioned before, the desorption temperature of the β state decreases strongly with increasing Sn concentration, while the desorption temperature of the α state is almost independent of the Sn concentration in the surface. Using Redhead [22] analysis, and assuming a preexponential factor of 10^{13} s^{-1} and first-order desorption kinetics, the desorption temperatures of the β_1 and β_2 states can be translated roughly to binding energies of 19.5 and 22 kcal/mol on Pt(111). The presence of Sn reduces the binding energy of the β state to 14 kcal/mol on the (2×2) alloy and 12 kcal/mol on the $\sqrt{3}$ alloy.

Fig. 6 shows an uptake plot for NO adsorption on the three surfaces. The NO TPD area can be converted to the NO coverage in the adsorbed monolayer by using the known saturation NO coverage on Pt(111) at 100 K, $\theta_{NO}^{Sat} = 0.5$ [4,9]. The presence of Sn reduces the NO saturation coverage to 0.4 on the (2×2) alloy and 0.3 on the $\sqrt{3}$ alloy. The slope of the uptake curve is proportional to the sticking coefficient of NO on the surface. As seen in Fig. 6, the slope is independent of NO coverage up to a NO coverage of 0.45 ML on Pt(111), 0.25 ML on the (2×2) alloy and 0.2 ML on the $\sqrt{3}$ alloy, indicating the importance of a precursor state in the adsorption kinetics on all three surfaces. Precursor-mediated ad-

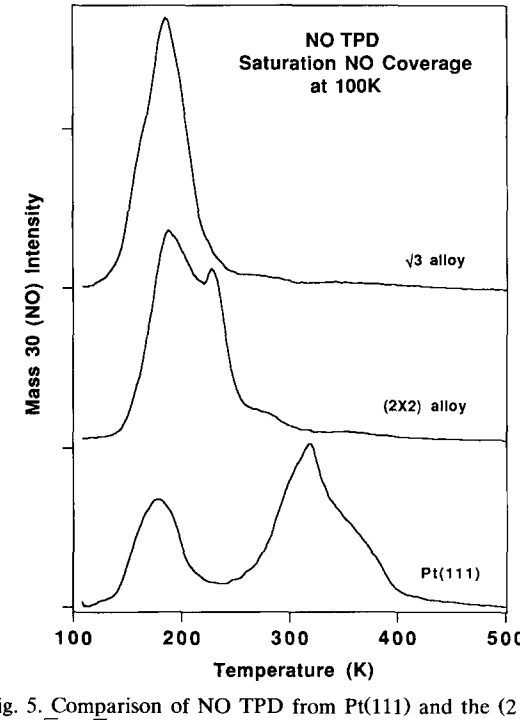

Fig. 5. Comparison of NO TPD from Pt(111) and the (2×2) and $(\sqrt{3} \times \sqrt{3})$R30°Sn/Pt(111) surface alloys.

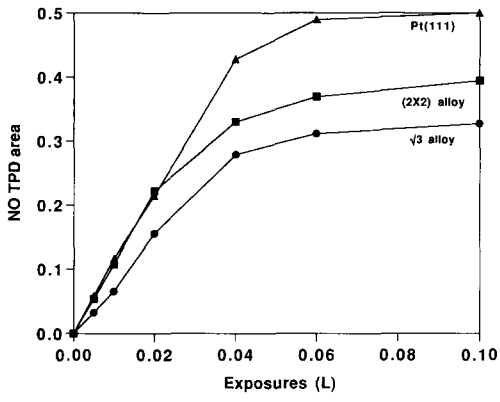

Fig. 6. NO uptake by the Sn/Pt(111) surface alloys compared to Pt(111) by using integrated NO TPD peak areas from Figs. 2–4.

sorption kinetics also was seen previously for NO on the Pt(111) surface [5,6,13]. Fig. 6 also shows that the initial sticking coefficient of NO on the (2×2) alloy is the same as on the Pt(111) surface, while a decreased initial sticking coefficient occurs on the $\sqrt{3}$ alloy. Using the well known initial sticking of NO on Pt(111) at 100 K, $S_0 = 0.9$ [5,6], the initial sticking coefficient of NO on the two surface alloys can be determined as 0.9 and 0.6, respectively.

3.2. LEED

We have studied NO adsorption using LEED on all three surfaces. Consistent with previous investigations [1,3,7], we found a (2×2) LEED pattern on the Pt(111) surface. We also found that this (2×2) LEED pattern exists over a wide range of NO coverages on the surface. Starting at 25% of saturation coverage, a sharp (2×2) LEED pattern was observed which showed almost no visual change with increasing NO coverage up to saturation. This indicates that an ordered (2×2) NO structure corresponding to a NO coverage of 0.25 ML is formed already at one-half NO saturation coverage. Further increasing the NO coverage either converts the (2×2) to a (2×1) structure, which still has a (2×2) LEED pattern because of the three different domains that will be present on the surface, or forces the excess NO to occupy different sites that also form a (2×2) structure. In both cases, the saturation coverage of NO on the surface will be 0.5 ML. This is consistent with the results of Gorte et al. [4] and Bartram et al. [9], but different than the result by Hayden [7] who estimated a NO saturation coverage of 0.25 ML.

Saturating the (2×2) surface alloy with NO at 100 K causes only an increase in the diffuse background. After the (2×2) alloy surface with a saturation NO coverage is annealed to 170 K, a sharp $(2\sqrt{3} \times 2\sqrt{3})$R30° LEED pattern was observed. This LEED pattern is schematically reproduced in Fig. 7. Dosing NO again at 100 K cannot remove this $(2\sqrt{3} \times 2\sqrt{3})$R30° LEED pattern. This indicates that the phase transition is correlated more with an ordering process during the annealing rather than desorption of excess NO on the surface.

No new LEED spots due to an ordered NO structure were ever observed on the $\sqrt{3}$ surface alloy under any conditions.

3.3. HREELS

HREELS spectra of saturation coverages of NO on Pt(111) and the (2×2) and $\sqrt{3}$ surface alloys are provided in Fig. 8. HREELS of NO on Pt(111) are characterized by two peaks in the low frequencies range (285 and 445 cm^{-1}) and two peaks at higher frequency (1515 and 1718 cm^{-1}). These observations are in good agreement with the results in the literature [1,2,9]. The peaks at 1515 and 1718 cm^{-1} have been assigned previously to the N–O vibration of NO adsorbed on a bridge site and linearly bonded NO adsorbed on an atop site, respectively [2,9]. The two peaks at

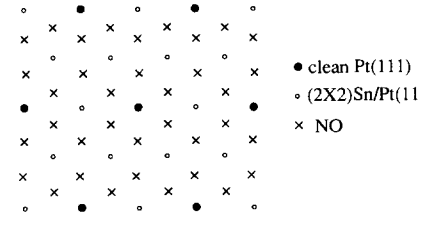

Fig. 7. LEED pattern observed after annealing a NO-saturated (2×2)Sn/Pt(111) surface to 170 K.

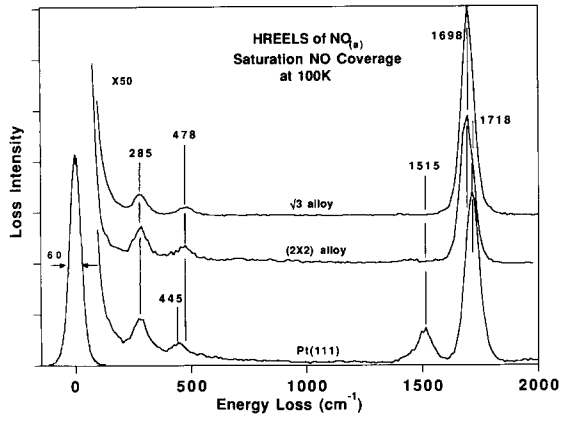

Fig. 8. HREELS spectra of NO saturation coverages on Pt(111) and the (2×2) and ($\sqrt{3} \times \sqrt{3}$)R30°Sn/Pt(111) surface alloys.

285 and 445 cm^{-1} have been correlated to the Pt–NO vibration [2,9]. These assignments are questionable however and we will discuss this point later.

Comparing NO adsorption on Pt(111) to the two Sn/Pt(111) surface alloys, the peak at 1515 cm^{-1} on Pt(111) disappears completely and the peak at 1718 cm^{-1} shifts to 1698 cm^{-1} on the two surface alloys. The single vibration at 1698 cm^{-1} suggests that all NO is adsorbed in the atop site on the two surface alloys. In contrast, both peaks at lower frequency are still seen on the two surface alloys. The peak at 285 cm^{-1} remains at the same frequency and an upward shift of 33 cm^{-1} is observed for the peak at 445 cm^{-1} on Pt(111) in going from Pt(111) to the two Sn/Pt(111) surface alloys. The presence of two vibrational peaks at lower frequency suggest a tilted adsorbed NO species on the two Sn/Pt(111) surface alloys. Because of the bent geometry, one of the two frustrated-rotational modes in the bending direction becomes dipole active. The bending mode of tilted NO adsorbed on the surface is well known to be around 500 cm^{-1} [9,23–25]. Our observation of a second peak in addition to the Pt–NO vibration in the lower frequency range proves that NO must be adsorbed as a tilted species on atop sites on the two surface alloys.

At lower NO coverage, the situation is slightly different. Fig. 9 shows this point as the HREELS spectra of 0.1 ML NO on Pt(111) and the (2 × 2) and $\sqrt{3}$ alloy surfaces are compared. The features on Pt(111) and the $\sqrt{3}$ alloy are the same as at NO saturation coverage except some small shifts of the peaks. On the (2 × 2) surface, however, a new peak at 1445 cm^{-1} is seen. From the vibrational frequency alone, this peak can be attributed to NO either on the three-fold hollow or the two-fold bridge site. It is possible that this peak is correlated to the small peak at 277 K (some kind of defect site) in the TPD spectra. But, the fact that the $\sqrt{3}$ alloy shows the same desorption peak with similar intensity and no loss peak is seen in the HREELS spectra of NO on the $\sqrt{3}$ alloy excludes this possibility. With increasing NO coverage, the peak at 1445 cm^{-1} on the (2 × 2) alloy disappears completely. This is consistent with the finding on Pt(111) that most bridge-bonded NO is converted to atop sites with increasing NO coverage [1,2,7].

We also observed NO-coverage dependent shifts of the N–O vibrational frequencies. In Fig. 10 we compare the frequency shift of the N–O vibration associated with 0.1 ML NO to that for saturation NO coverage on Pt(111) and the (2 × 2) and $\sqrt{3}$ alloy surfaces. It can be seen from Fig. 10 that the two alloy surfaces show a much higher coverage-dependent shift of the NO vibrational

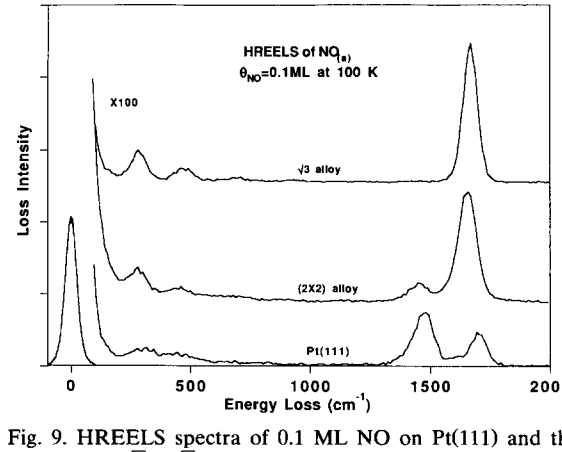

Fig. 9. HREELS spectra of 0.1 ML NO on Pt(111) and the (2×2) and ($\sqrt{3} \times \sqrt{3}$)R30°Sn/Pt(111) surface alloys.

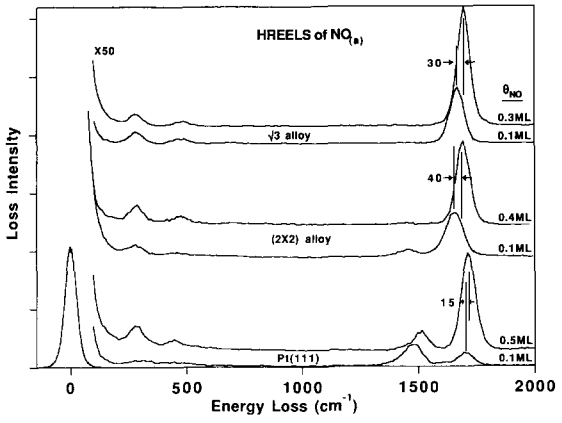

Fig. 10. Comparison of the coverage dependent shift of the N–O stretching vibrational frequency on Pt(111) and the (2×2) and ($\sqrt{3} \times \sqrt{3}$)R30°Sn/Pt(111) surface alloys.

frequency than the Pt(111) surface. The coverage dependent shift has been attributed in the past to either a dipole or static shift [26]. A dipole shift is a result of the interaction between the dipole of a molecule with the dipole and the image dipole of its neighbors. A static shift has its origin in an electrostatic interaction and the chemical modification of the surface electronic structure by the adsorbed molecules. The coverage dependent frequency shift of NO on the Pt(111) surface has been studied previously by Hayden [7] with infrared reflection absorption spectroscopy (IRAS). In an isotopic dilution experiment using $N^{14}O$ and $N^{15}O$, he was able to separate out the dipole and static contributions to the coverage dependent frequency shift. NO in the atop site has a dipole shift of 33 cm^{-1} and a static shift of -13 cm^{-1} at saturation coverage. Consistent with his result, we found the coverage dependent frequency shift on Pt(111) is 15 cm^{-1} upward by increasing the coverage from 0.1 ML to saturation coverage. On the surface alloys we have a strongly reduced binding energy of NO as indicated by TPD. Therefore, one would expect a much smaller static shift. This was observed and, as a result, the two surface alloys show a larger coverage dependent frequency shift compared to Pt(111).

4. Discussion

4.1. Adsorption site

The adsorption of NO on Pt(111) and modified Pt(111) surfaces has been studied previously using LEED, AES, UPS, XPS, TPD, HREELS and IR [1–14]. The NO adsorption kinetics has been studied also using molecular beam techniques and sticking coefficient measurements [5,6,12,13]. NO is adsorbed molecularly on the Pt(111) surface. The small amount of dissociative adsorption seen in early studies can be attributed to adsorption on defect sites which are correlated to NO desorption at a temperature higher than 450 K. A similar higher temperature desorption state that is correlated to defect sites has been seen also for CO on Pt(111). We cannot populate this state on our surface and consequently no NO dissociation was found in our TPD experiments.

There is some controversy regarding the adsorption sites of NO on Pt(111). Two species have been consistently found with increasing NO coverage in HREELS investigations. Ibach and Lehwald [1] assigned the species at low NO coverage with an N–O vibrational frequency of 1515 cm^{-1} to an NO monomer on the atop site and the species at higher coverage with a frequency of 1717 cm^{-1} to a dimer. Gland and Sexton [2] reassigned the two species corresponding to 1490 and 1710 cm^{-1} to NO adsorbed on the bridge site and linearly bonded on the atop site, respectively. They also found small concentrations of a species that desorbs at higher temperature in TPD which has peaks in HREELS at 1600 and 1820 cm^{-1}. By using IR and well-known CO adsorption bands on the defect sites on Pt(111), Agrawal and Trenary [10] were able to assign the higher temperature TPD peaks to NO adsorbed on defect sites. Hayden's [7] studies of NO adsorption on Pt(111) using IRAS and isotopic mixtures of $N^{14}O$ and $N^{15}O$ are quite illuminating. For a monomer/dimer model, one would expect to observe a doublet for the monomer and a triplet for the dimer. For an atop/bridge site model, one only would observe two doublets for the two sites. The fact that only two doublets

were observed at any isotopic mixture ratio led Hayden to conclude that NO is adsorbed on the bridge and atop site (linearly bonded). Finally, Bartram et al. [9] correlated the two species observed in HREELS to the desorption peaks β_1 and β_2 by using surface oxygen to selectively block one species.

Our experimental results are consistent with the assignment of two peaks in HREELS to two different adsorption sites rather than to a monomer and dimer model. However, the assignment of the peaks in the HREELS to the linear atop and bridge sites seems to us to be inconsistent with some of the experiment results. The NO coverage dependent HREELS experiments by Ibach [1] et al. and Gland et al. [2] both show that only peaks at 285 and 1515 cm^{-1} exist at low NO coverage. With increasing coverage, the peaks at 445 and 1718 cm^{-1} appear. If one assigns the peaks at 1515 and 1718 cm^{-1} to NO adsorbed on the bridge and linear atop site, the peak at 285 cm^{-1} must be assigned to the Pt–NO vibration of NO on the bridge site and the peak at 445 cm^{-1} to the corresponding mode for the atop site. On both Sn/Pt(111) alloys, the Pt–NO vibration of NO on the atop site is 285 cm^{-1}. It is not clear why the two Pt–NO vibrational frequencies for the atop site on Pt(111) and the Sn/Pt(111) alloys would be different. An alternative assignment of the spectrum on Pt(111) is that the peak at 1718 cm^{-1} is due to bent NO adsorbed on the atop site rather than NO linearly bound on the atop site. Consequently, the peak at 445 cm^{-1} can be assigned to the Pt–NO bending mode and the peak at 285 cm^{-1} to the Pt–NO vibration of both species. This assignment is consistent with a recent ab initio GVB/CI calculation by Smith and Carter [11] showing that NO bound to a single Pd or Pt metal atom or ion always prefers a bent structure.

The assignment of the peak at 1515 cm^{-1} to NO adsorbed on the bridge site is based solely on the comparison of the vibrational frequency with nitrosyl complexes. Unfortunately, the N–O vibrational frequency of three-fold bonded NO can be as high as 1545 cm^{-1} and of two-fold bridge bonded NO as low as 1480 cm^{-1} [10] and so the assignment of the peak at 1515 cm^{-1} is difficult. Additional spectroscopic investigations are needed. In a recent dynamical LEED experiment, Materer et al. [14] reassigned all NO adsorption previously thought to occur on the two-fold bridge site to the three-fold hollow site. However, they did not report the NO coverage used in their experiments. (They dosed 1 L NO and annealed to 250 K to produce a (2×2) LEED pattern.) In our experiments, we have shown that the β_2 state, which will be populated first and has a vibrational mode at 1515 cm^{-1}, can also produce a (2×2) LEED pattern. Therefore, we assume that the dynamical LEED study only involved the β_2 state. If that is the case, the peak at 1515 cm^{-1} can be attributed to NO adsorbed on the three-fold hollow site.

At small NO coverage, the three-fold hollow site also can be populated on the (2×2) alloy in addition to the atop site, while NO on the atop site is the only species on the $\sqrt{3}$ alloy. This is consistent with the fact that the $\sqrt{3}$ alloy surface does not have any three-fold hollow sites containing only Pt atoms. Going to higher NO coverage, the tilted NO adsorbed on the atop site remains the only species on both Sn/Pt(111) surface alloys. This is due to the destabilization of NO adsorbed on three-fold hollow sites with increasing NO coverage. Similar effects were also observed for NO on Pt(111).

NO adsorbed in a disordered fashion on the (2×2) surface alloy at 100 K. However, annealing to 170 K causes ordering of the NO layer producing a $(2\sqrt{3} \times 2\sqrt{3})R30°$ surface net. HREELS shows only one type of NO species adsorbed on atop sites in a tilted geometry. From TPD, the coverage of NO is determined to be ~ 0.4 ML. Combining these results, we propose a structural model for NO on the (2×2) alloy as shown in Fig. 11. The coverage of our proposed structure is 0.33 ML, close to the coverage determined by the TPD experiment. This structure is also consistent with the finding of LEED and HREELS. Since NO exists "pairwise" on the surface, one might think of dimer formation. However, the distance between two adjacent atop sites is 0.277 nm, much larger than the N–N distance in $(NO)_2$ which is about 0.218 nm. Therefore, the interaction between two NO near-

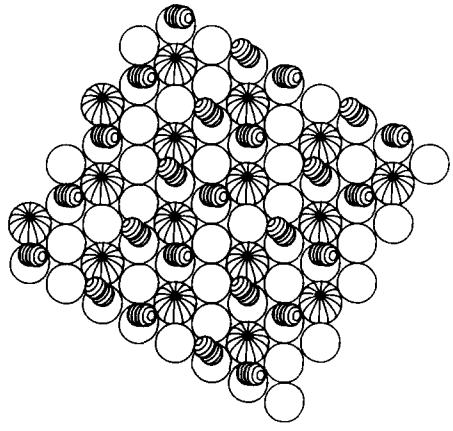

Fig. 11. Proposed structure of the $(2\sqrt{3} \times 2\sqrt{3})$R30°-NO adsorbate layer on the (2×2)Sn/Pt(111) surface alloy.

est neighbors should be much weaker than in the dimer, and it could even be repulsive.

4.2. Adsorption kinetics

The adsorption kinetics of NO on the Pt(111) surface has been a subject of both theoretical [12] and experimental investigations [5,6,13]. The initial sticking coefficient of NO on Pt(111) has been found to be very high, $S_0 = 0.9$. The dependence of the sticking coefficient on the NO coverage is dominated by the presence of an extrinsic precursor state. Our experimental result on Pt(111) is in good agreement with previous measurements. We found a constant value of S independent of NO coverage, up to a NO coverage of 0.45 ML, indicating precursor-mediated adsorption kinetics.

The presence of Sn in the Pt(111) surface influences the initial sticking coefficient and saturation coverage of NO differently. This is clearly shown in Fig. 12. A linear scaling of the saturation coverage of NO with the Sn concentration in the surface layer would describe our data reasonably well. By contrast, the initial sticking coefficient is not affected by the Sn concentration (0.25 ML) in the (2×2) surface alloy. Increasing the Sn concentration to 0.33 ML causes the initial sticking coefficient to drop to 0.6.

Similar effects have been seen for many bimetallic surfaces and are general phonemena on bimetallic and modified surfaces. Recently we have pointed out that the Langmuir isotherm cannot be used to describe the dependence of initial sticking coefficient on the modifier coverage [27]. Incorrect results are often obtained when the initial sticking coefficient is modelled by using a simple site-blocking equation such as $S_M = S(1 - m\theta_M)$, where S and S_M are the sticking coefficients on the clean surface and on the surface containing a modifier (second metal component), respectively, θ_M is the modifier coverage, and m is the parameter describing how many sites are blocked by one atom of the modifier. (This equation might still be useful to describe the dependence of the saturation coverage on the modifier concentration however.) The physical reason for the failure of the Langmuir isotherm is the presence of the "modifier precursor" which exists on top of the modifier. If one assumes the presence of a precursor state "on top" of NO molecules to explain the independence of the sticking coeffi-

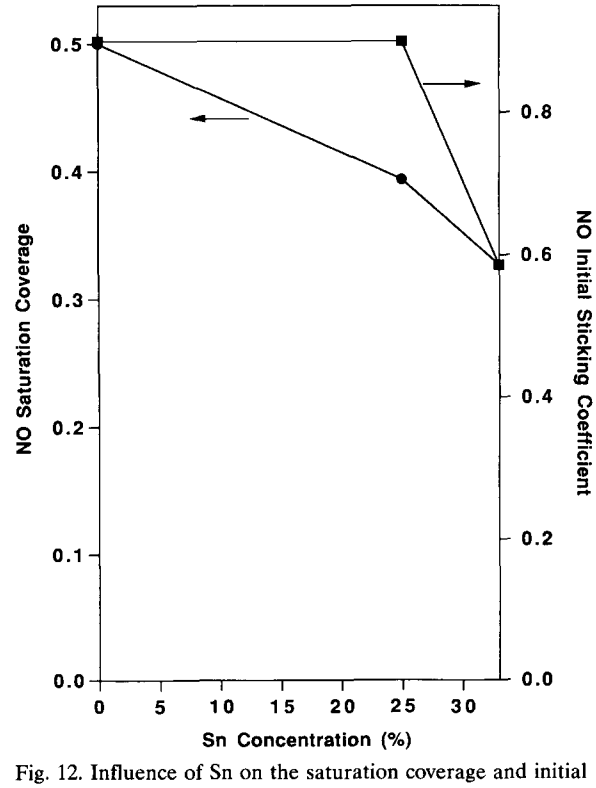

Fig. 12. Influence of Sn on the saturation coverage and initial sticking coefficient of NO on the Pt(111) surface.

cient on the NO coverage on Pt(111), it is only reasonable to recognize that a precursor state exists on top of Sn also. The presence of this modifier precursor prevents a linear decrease of the sticking coefficient with increasing Sn coverage just as in the case of Pt(111) where the extrinsic precursor prevents a linear decrease of the sticking coefficient with increasing NO coverage.

These results demonstrate that the presence of Sn has a strong influence on the adsorption kinetics by introducing a new adsorption/desorption pathway, in addition to altering the chemical nature of the Pt(111) surface and the energetics of adsorption. The important role played by the modifier precursor must be taking into account in order to fully understand the chemistry of these Pt–Sn surface alloys and other bimetallic surfaces.

4.3. Bonding

The presence of Sn has a strong electronic effect on NO adsorption on Pt(111) as indicated by the strong reduction in NO adsorption energy with increasing Sn concentration. It is especially interesting to compare these results with those of CO adsorption on the same Sn/Pt(111) surface alloys [21]. In contrast to NO, the binding energy of CO only decreases slightly from the Pt(111) surface ($E_{des} = 25$ kcal/mol for bridge-bonded and 29 kcal/mol for atop CO) to the (2×2) ($E_{des} = 25$ kcal/mol) and $\sqrt{3}$ ($E_{des} = 24$ kcal/mol) surface alloys. Both bridge-bonded and atop CO can be populated on all three surfaces with a ratio corresponding to the site ratio of each surface. Sn has almost no effect on the CO adsorption energetics or site occupancy.

How can we rationalize this difference between CO and NO? The bonding of NO on transition metals has been previously described by Bartram, Koel and Carter [9]. Similar to that for CO, the NO surface chemical bond can be described as involving σ donation and π back-donation. However, the presence of one more electron in the $2\pi^*$ orbital compared to CO enables NO to be bound to the surface in completely different manner. By utilizing this single

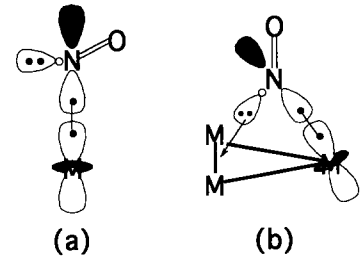

Fig. 13. Schematic picture of NO bonding on transition metal surfaces.

unpaired electron in the $2\pi^*$ orbital, NO can form a covalent bond with the surface. A schematic view of the bonding configuration of NO adsorbed at atop sites in a bent geometry and linearly bonded at three-fold hollow sites is shown in Fig. 13. This view is adapted from Ref. [9] and a more detailed discussion can be found there. For our purposes, we only want to point out the obvious importance of the covalent bond in the bonding of NO to transition metals. Recently, Smith and Carter [11] studied the interaction of CO and NO with single Pt atoms using an ab initio generalized valence bond and correlation-consistent configuration interaction (GVB/CI) approach. They concluded that PtNO is bent with the dominant bonding involving a covalent σ bond between a singly occupied metal d_σ orbital and the singly occupied NO $2\pi^*$ orbital. Consistently, we argue in favor of NO adsorption on atop sites on Pt(111) in a bent configuration. Bartram et al. [9] also concluded from their experiments that the covalent σ (atop site) or π (three-fold hollow site) bond formed to the platinum surface using the $2\pi^*$ electron in NO dominates the strength of the Pt–NO bond. In order to form a covalent metal–NO bond, the presence of a singly occupied metal orbital is essential. By contrast, the presence of an empty metal σ orbital for donation from the 5σ orbital of CO and doubly occupied metal d_π orbitals for π back-bonding into the empty CO $2\pi^*$ orbital (the dominant interactions) are important to form the metal–CO bond. Very different parts of the electronic structure at the surface are utilized for the CO– and NO–metal bonds. *The presence of Sn obviously reduces*

the ability of the substrate to form covalent bonds, but does not substantially change the capability of the substrate to participate in π back-bonding. This can be correlated to changing either the electron density in individual bands or the energy levels of different bands by alloying Pt with Sn. A definitive answer requires more detailed spectroscopic investigations using techniques such as ARUPS and IPS.

5. Conclusion

The presence of Sn within the surface layer of Pt–Sn alloys has a strong effect on the thermodynamics of NO adsorption. The binding energy of NO is strongly reduced by alloying Sn in the Pt(111) surface, in contrast to that for CO. This is mainly due to selective modification of the electronic structure of the Pt(111) surface by the addition of Sn and the different bonding interactions responsible for chemisorption of NO and CO. NO is adsorbed mainly in a bent configuration on atop sites on both Sn/Pt(111) surface alloys studied. At small NO coverages, a small concentration of NO is adsorbed in the three-fold hollow sites on the (2×2) surface alloy. Based on TPD, LEED and HREELS results, a structure for the $(2\sqrt{3} \times 2\sqrt{3})$R30°-NO adsorbate layer on the (2×2) alloy has been proposed. The presence of Sn in the surface alloys has much less affect on the NO adsorption kinetics than might be expected from simple site-blocking arguments due to the importance of a modifier precursor state.

Acknowledgments

This work was supported by the US Department of Energy, Office of Basic Energy Sciences, Chemical Sciences Division. We thank Professor Emily A. Carter for several useful discussions.

References

[1] H. Ibach and S. Lehwald, Surf. Sci. 76 (1978) 1.
[2] J.L. Gland and B.A. Sexton, Surf. Sci. 94 (1980) 353.
[3] T.H. Lin and G.A. Somorjai, Surf. Sci. 107 (1981) 573.
[4] R.J. Gorte, L.D. Schmidt and J.L. Gland, Surf. Sci. 109 (1981) 367.
[5] C.T. Campbell, G. Ertl and J. Segner, Surf. Sci. 115 (1982) 309.
[6] J.A. Serri, M.J. Cardillo and G.E. Becker, J. Chem. Phys. 77 (1982) 2175.
[7] B.E. Hayden, Surf. Sci. 131 (1983) 419.
[8] M. Kiskinova, G. Pirug and H.P. Bonzel, Surf. Sci. 136 (1984) 285.
[9] M.E. Bartram, B.E. Koel and E.A. Carter, Surf. Sci. 219 (1989) 467.
[10] V.K. Agrawal and M. Trenary, Surf. Sci. 259 (1991) 116.
[11] G.W. Smith and E.A. Carter, J. Phys. Chem. 95 (1991) 2327.
[12] C. Haug, W. Brenig and T. Brunner, Surf. Sci. 265 (1992) 56.
[13] J.K. Brown and A.C. Luntz, Chem. Phys. Lett. 204 (1993) 451.
[14] N. Materer, A. Barbieri, D. Gardin, U. Starke, J.D. Batteas, M.A. Van Hove and G.A. Somorjai, Phys. Rev. B 48 (1993) 2859.
[15] J.H. Sinfelt, Bimetallic Catalysis: Discoveries, Concepts, and Applications (Wiley, New York, 1983).
[16] C.T. Campbell, Ann. Rev. Phys. Chem. 41 (1990) 775.
[17] C.T. Campbell, G. Ertl, H. Kuipers and J. Segner, Surf. Sci. 107 (1981) 220.
[18] M.T. Paffett and R.G. Windham, Surf. Sci. 208 (1989) 34.
[19] S.H. Overbury, D.R. Mullins, M.T. Paffett and B.E. Koel, Surf. Sci. 254 (1991) 45.
[20] A. Atrei, U. Bardi, J.X. Wu, E. Zanazzi and G. Rovida, Surf. Sci. 290 (1993) 286.
[21] M.T. Paffett, S.C. Gebhard, R.G. Windham and B.E. Koel, J. Phys. Chem. 94 (1990) 6831.
[22] P. Redhead, Vacuum 12 (1962) 203.
[23] G. Pirug, H.P. Bonzel, H. Hopster and H. Ibach, J. Chem. Phys. 71 (1979) 593.
[24] S. Lehwald, J.T. Yates, Jr. and H. Ibach, in: Proc. IVC-8 and ECOSS-3, Cannes (1980) [Suppl. Le Vide, Les Couches Minces 201 (1980) 221].
[25] J.F. Wendelken, Appl. Surf. Sci. 11/12 (1982) 172.
[26] R.F. Willis, A.A. Lucas and G.D. Mahan, in: The Chemical Physics of Solid Surfaces and Heterogeneous Catalysis, Vol. 2, Eds. D.A. King and D.P. Woodruff (Elsevier, Amsterdam, 1982) p. 59.
[27] C. Xu and B.E. Koel, J. Chem. Phys. 100 (1994) 664.